Self-calibration algorithm under varying cameras using the linear projective reconstruction method

Jong-Eun Ha
Department of Mechanical Engineering, KAIST
373-1, Kusung-Dong, Yusong-Gu, Taejon, South Korea
jeha@cais.kaist.ac.kr

Jin-Young Yang
Communication Network Lab.,Samsung Electronics co.
416,Maetan-3Dong,Paldal-Gu,Suwon,Kyungki-Do,Korea
yjymail@samsung.co.kr

In-So Kweon
Department of Electrical Engineering, KAIST
373-1,Kusung-Dong,Yusong-Gu,Taejon,South Korea
iskweon@cais.kaist.ac.kr

ABSTRACT

We present a practical self-calibration algorithm that only requires a linear projective reconstruction. Recently, many self-calibration algorithms that use only the information in the image have been proposed. But most algorithms require bundle adjustments in the projective reconstruction or in the nonlinear minimization. We overcome the sensitivity of the self-calibration algorithms due to the image noises by adding another constraint on the position of the principal point. We also propose a linear initialization method based on the property of the absolute quadric. Experimental results using real and synthetic images demonstrate the feasibility of the proposed algorithm.

Keywords: Self-calibration, 3D reconstruction, absolute quadric

1. INTRODUCTION

The metric reconstruction of a given scene from image streams is an important step in computer vision. Traditional methods first calibrate a camera using a calibration object, and then acquire a metric structure of a given scene using the correspondence between images. These approaches need the calibration object in any given scene, thus their application areas are limited.

Recently self-calibration (or auto-calibration) algorithms have been actively researched to relax the requirement of the calibration box in the scene. Self-calibration algorithms calibrate the camera using only the information on the images. Earlier algorithms for self-calibration deal with situations where the intrinsic parameters of cameras remain constant in the sequences. Most of these methods use the property of the absolute conic that remains invariant under all Euclidean transformations.

Faugeras et al. [1] proposed a self-calibration algorithm which uses the Kruppa equation. It enforces that the planes through two camera centers which are tangent to the absolute conic should also be tangent to both of its images. Hartley [2] proposed another method based on the minimization of the difference between the internal camera parameters for the different views. Polleyfeys et al. [3] proposed a stratified approach that first recovers the affine geometry using the modulus constraint and then recovers the Euclidean geometry through the absolute conic. Heyden and Åström [4], Triggs [5] and Pollefeys & Van Gool [6] use explicit constraints that relate the absolute conic to its images. These formulations are especially interesting since they can easily be extended to deal with the varying internal camera parameters.

Recently self-calibration algorithms that can deal with the varying intrinsic parameters of the camera were proposed. Heyden and Åström [7] proposed a self-calibration algorithm that uses explicit constraints from the assumption of the camera intrinsic parameters. They proved that self-calibration is possible under varying cameras when the assumptions that the aspect ratio was known and no skew establishes about the camera. They solved the problem using the bundle adjustment that requires simultaneous minimization on the all reconstructed points and cameras. Moreover, the initialization problem was not properly presented. Bougnoux [8] proposed a practical self-calibration algorithm that used the constraints derived from Heyden and Åström [7]. He proposed the linear initialization step in the nonlinear minimization. He used the bundle adjustment in the projective reconstruction step. Similarly, Pollefeys et al. [9] proposed a versatile self-calibration method that can deal with a number of types of constraints about the camera. They showed a specialized version for the case where the focal length varies, possibly also the principal point.

We propose a practical self-calibration algorithm that only requires a linear projective reconstruction. We overcome the sensitivity of the algorithm partially due to the linear projective reconstruction by adding a new constraint on the principal point. We also propose a new linear initialization method based on the property of the absolute quadric.

2. THE SELF-CALIBRATION ALGORITHM

In this section, we review the self-calibration algorithm that appears in [8]. The process of projection of a point in 3D

to the image plane can be represented as the following sequential steps:

$$\mathbf{P}_{euc} = \mathbf{A}\mathbf{P}_0\mathbf{T} = \begin{bmatrix} a_u & g & u_0 \\ 0 & a_v & v_0 \\ 0 & 0 & 1 \end{bmatrix} \begin{bmatrix} 1 & 0 & 0 & 0 \\ 0 & 1 & 0 & 0 \\ 0 & 0 & 1 & 0 \end{bmatrix} \begin{bmatrix} \mathbf{R} & \mathbf{t} \\ \mathbf{0}_3^T & 1 \end{bmatrix} \quad (1)$$

where $\mathbf{T}$ represents the transformation of coordinate systems from world to the camera-centered system, $\mathbf{P}_0$ is the perspective projection and $\mathbf{A}$ consists of the intrinsic parameters of camera.

We use the following assumptions about the intrinsic parameters of camera

$$\begin{aligned} g &= 0 \\ a_u &= a_v \end{aligned} \quad (2)$$

It is well known that we can reconstruct a scene up to the projective transformations using only corresponding points on the images [10, 11]. This can be represented as:

$$\tilde{\mathbf{m}}_j^i \cong \mathbf{P}_{proj}^i \tilde{\mathbf{M}}_j^{proj} = \mathbf{P}_{proj}^i \mathbf{Q}\mathbf{Q}^{-1}\tilde{\mathbf{M}}_j^{proj} \quad (3)$$

where $\tilde{\mathbf{m}}_j^i$ is the j-th point in the i-th image, $\mathbf{P}_{proj}^i$ is a projective projection matrix of the i-th image and $\tilde{\mathbf{M}}_j^{proj}$ is a projective structure of scene point corresponding to the image point $\tilde{\mathbf{m}}_j^i$. The projective structure $\tilde{\mathbf{M}}_j^{proj}$ is related to the metric structure by a projective transformation matrix $\mathbf{Q}$. In Eq. (3), any nonsingular matrix $\mathbf{Q}$ satisfies the above relation, so there can be many projective reconstructions. There exists a unique $\mathbf{Q}$ matrix that transforms the projective structure to a metric structure of a given scene. Finding this $\mathbf{Q}$ matrix is calibration process. We can obtain the Euclidean projection matrix and the metric structure of a scene using this unique $\mathbf{Q}$ matrix.

$$\begin{aligned} \mathbf{P}_{euc}^i &\cong \mathbf{P}_{proj}^i \mathbf{Q} \\ \tilde{\mathbf{M}}_j^{euc} &\cong \mathbf{Q}^{-1}\tilde{\mathbf{M}}_j^{proj} \end{aligned} \quad (4)$$

In general, under the pinhole camera model, we can set the projective projection matrix of the first camera as $\mathbf{P}_{proj}^1 = [\mathbf{I}_3 \quad \mathbf{0}_3]$. We have the Euclidean projection matrix of the first camera $\mathbf{P}_{euc}^1 = [\mathbf{A}_1 \quad \mathbf{0}_3]$ if we set the world coordinate at the optical center of the first camera. By substituting these projection matrices in Eq. (4), we obtain:

$$\begin{aligned} \mathbf{P}_{euc}^1 \cong \mathbf{P}_{proj}^1\mathbf{Q} &\Leftrightarrow [\mathbf{A}_1 \quad \mathbf{0}_3] \cong [\mathbf{I} \quad \mathbf{0}_3]\mathbf{Q} \\ &\Leftrightarrow \exists(\mathbf{q}, q_{44}) \mid \mathbf{Q} \cong \begin{bmatrix} \mathbf{A}_1 & \mathbf{0}_3 \\ \mathbf{q}^T & q_{44} \end{bmatrix} \end{aligned} \quad (5)$$

Here, $\mathbf{Q}$ is defined up to a scale and it can be represented as

$$\mathbf{Q} = \begin{bmatrix} f & 0 & u_0 & 0 \\ 0 & f & v_0 & 0 \\ 0 & 0 & 1 & 0 \\ q_1 & q_2 & q_3 & 1 \end{bmatrix} = \begin{bmatrix} \mathbf{A}_1 & \mathbf{0}_3 \\ \mathbf{q}^T & 1 \end{bmatrix} \quad (f \equiv a_u, a_v) \quad (6)$$

Now $\mathbf{Q}$ matrix contains six unknowns. Next we review the constraint for obtaining $\mathbf{Q}$ matrix.

If we set $\mathbf{P}_{euc}^i$,

$$\mathbf{P}_{euc}^i \cong \mathbf{P}_{proj}^i\mathbf{Q} = \begin{bmatrix} \mathbf{p}_1^{iT} & \\ \mathbf{p}_2^{iT} & \mathbf{t}_i \\ \mathbf{p}_3^{iT} & \end{bmatrix} \quad (7)$$

then we have the following constraint for the Euclidean projection matrix, $\mathbf{P}_{euc}$ [12].

$$\begin{aligned} g = 0 &\Leftrightarrow (\mathbf{p}_1 \times \mathbf{p}_3) \bullet (\mathbf{p}_2 \times \mathbf{p}_3) = 0 \\ a_u = a_v &\Leftrightarrow \|\mathbf{p}_1 \times \mathbf{p}_3\| = \|\mathbf{p}_2 \times \mathbf{p}_3\| \end{aligned} \quad (8)$$

These equations give two constraints for the unknown $\mathbf{Q}$ matrix for each camera and we can obtain the solution using at least 4 images. The resulting problem can be formulated as the nonlinear estimation that minimizes Eq. (8) for each camera.

3. A NEW LINEAR METHOD FOR THE INITIALIZATION

The nonlinear estimation problem needs some initial values of unknown parameters. The initial values of u_0, v_0 are set as the image center of the first image. Bougnoux [8] proposed the following initialization method for f using the Kruppa equation.

$$\begin{aligned} &\mathbf{F}\mathbf{K}\mathbf{F}^T \cong [\mathbf{e}']_\times \mathbf{K}' [\mathbf{e}']_\times, \\ &where\, \mathbf{K} = \mathbf{A}\mathbf{A}^T, \mathbf{K}' = \mathbf{A}'\mathbf{A}'^T \end{aligned} \quad (9)$$

where $\mathbf{F}$ is the Fundamental matrix, $\mathbf{A}$ and $\mathbf{A}'$ are the matrices that contain the intrinsic parameters of the first and the second camera and $\mathbf{e}'$ is the epipole of the second camera. If we remove the scale using $\tilde{\mathbf{F}} = l\mathbf{F}, \tilde{\mathbf{e}}' = m\mathbf{e}'$ we have the Kruppa equation:

$$\tilde{\mathbf{F}}\mathbf{K}\tilde{\mathbf{F}}^T = x^2 [\tilde{\mathbf{e}}']_\times \mathbf{K}' [\tilde{\mathbf{e}}']_\times, \text{ where } x^2 = \frac{l^2}{m^2} \quad (10)$$

Bougnoux [8] proposed the following closed-form solution for the initial value of f using Eq. (10).

$$f = \sqrt{-\frac{\mathbf{p}'^T [\tilde{\mathbf{e}}']_\times \tilde{\mathbf{I}} \tilde{\mathbf{F}} \mathbf{p}\mathbf{p}^T \tilde{\mathbf{F}}^T \mathbf{p}'}{\mathbf{p}'^T [\tilde{\mathbf{e}}']_\times \tilde{\mathbf{I}} \tilde{\mathbf{F}} \tilde{\mathbf{I}} \tilde{\mathbf{F}}^T \mathbf{p}'}}, \text{ where } \tilde{\mathbf{I}} = \begin{bmatrix} 1 & 0 & 0 \\ 0 & 1 & 0 \\ 0 & 0 & 0 \end{bmatrix} \quad (11)$$

where $\mathbf{p} = (u_0, v_0, 1)^T$, $\mathbf{p}' = (u_0', v_0', 1)^T$. He also presented a method to determine the initial values $(q_1, q_2, q_3)^T$ using the property of orthogonality of the rotation matrix.

In this paper we propose a new method for the initial values based on the invariancy of the absolute quadric. Our method can recover the initial values linearly.

$$\omega = \mathbf{A}\mathbf{A}^T = \mathbf{P}_{euc}\Omega\mathbf{P}_{euc}^T, \; where\, \Omega = \begin{bmatrix} \mathbf{I}_3 & \mathbf{0}_3 \\ \mathbf{0}_3^T & 0 \end{bmatrix} \quad (12)$$

If we apply $\mathbf{P}_{euc}^i \cong \mathbf{P}_{proj}^i\mathbf{Q}$ to Eq. (12) we have

$$\begin{aligned}\mathbf{A}_i\mathbf{A}_i^T &= \mathbf{P}_{euc}^i\Omega\mathbf{P}_{euc}^{iT}\\ &= \mathbf{P}_{proj}^i(\mathbf{Q}\Omega\mathbf{Q}^T)\mathbf{P}_{proj}^{iT}\\ &= \mathbf{P}_{proj}^i\Omega'\mathbf{P}_{proj}^{iT}\end{aligned} \quad (13)$$

Eq. (13) can be represented as:

$$l_i\begin{bmatrix} f_i^2+u_0^2 & u_0v_0 & u_0\\ u_0v_0 & f_i^2+v_0^2 & v_0\\ u_0 & v_0 & 1\end{bmatrix} =$$

$$\mathbf{P}_{proj}^i\begin{bmatrix} f_1^2+u_0^2 & u_0v_0 & u_0 & f_1q_1+u_0q_3\\ u_0v_0 & f_1^2+v_0^2 & v_0 & f_1q_2+v_0q_3\\ u_0 & v_0 & 1 & q_3\\ f_1q_1+u_0q_3 & f_1q_2+v_0q_3 & q_3 & \|\mathbf{q}\|^2\end{bmatrix}\mathbf{P}_{proj}^{iT} \quad (14)$$

$$(a_1 = f_1q_1+u_0q_3, a_2 = f_1q_2+v_0q_3, a_3 = q_3, \|\mathbf{a}\|^2 = \|\mathbf{q}\|^2)$$

From the left-hand side of Eq. (14), we obtain $w_{11}-u_0^2/l_i = w_{22}-v_0^2/l_i$, $w_{12}=w_{21}$, $w_{13}=w_{31}$, and $w_{23}=w_{32}$. If we impose these equations on the right-hand side, this yields 4(n-1) linear equations in $f_1^2, a_1, a_2, a_3, \|\mathbf{a}\|^2$. If we remove $\|\mathbf{a}\|^2$ in the given equations, we have 3(n-1) linear equations in f_1^2, a_1, a_2, a_3. We assume that the intrinsic parameters are constant to get initial parameters. We also assume the principal point of the first camera as the image center. Under these assumptions we have four unknowns f_1, q_1, q_2, q_3 that can be obtained if we use more than three images through a least-squares estimation.

4. ADDING ANOTHER CONSTRAINT IN THE MINIMIZATION

We add another constraint to improve the behavior of the algorithm in the nonlinear minimization. We observed that the algorithm often gives some erroneous results when we only use the two constraints of Eq. (8). (This will be later explained in Section 5.)

The accuracy of the algorithm depends on the accuracy of the projective reconstruction. We used the simple linear method of Hartley [13] for the projective reconstruction, which gives a comparable result to that of nonlinear minimization under the Gaussian noise distribution. In spite of the small residual in the projective reconstruction the algorithm often gives a false result as noise level increases while the residual of the nonlinear minimization decreased. This is due to the inability of the two constraints to constrain the solution space in the meaningful range when the noise perturbs the projective projection matrices. Each constraint is a 4th order polynomial so the algorithm is very sensitive to the noise.

We partially overcome this problem by adding another constraint on the minimization. This is based on the experimental observations of the behavior of the algorithm that uses the constraints of Eq. (8). Among the six unknowns the principal point was most sensitive in the nonlinear minimization. Therefore it is necessary to constrain the position of the principal point in a restricted area to obtain a meaningful solution. We add the following constraint on the principal point.

$$\begin{aligned}\tilde{u}_0 - \hat{u}_0 &= 0\\ \tilde{v}_0 - \hat{v}_0 &= 0\end{aligned} \quad (15)$$

where $\tilde{u}_0, \tilde{v}_0$ is the image center of the first camera and $\hat{u}_0, \hat{v}_0$ is the estimated principal point in the minimization process.

We do not fix the value of the principal point of the first camera as the known value of the image center of the first image. This gives also a bad behavior in the minimization process.

The overall structure of the self-calibration algorithms is as follows:

(a) Find the projection matrix $\mathbf{P}_{proj}^i$ by projective reconstruction between images, e.g., 1-2, 1-3, ..,.
(b) Transform the projective reconstruction of (a) to have an equal basis in P^3
(c) Obtain some initial values of the unknowns using the linear method.
(d) Obtain a 4X4 homography Q through the nonlinear minimization.
(e) Recover the Euclidean projection by $\mathbf{P}_{euc}^i \cong \mathbf{P}_{proj}^i\mathbf{Q}$
(f) Recover the Euclidean structure by $\tilde{\mathbf{M}}_j^{euc} \cong \mathbf{Q}^{-1}\tilde{\mathbf{M}}_j^{proj}$

The step (b) is necessary because Eq. (3) establishes under an equal basis in P^3. We use the method proposed by Csurka & Horaud [14] to transform the projective reconstruction to have an equal basis in P^3.

5. EXPERIMENTAL RESULTS

5. 1 EXPERIMENTAL RESULTS USING SYNTHETIC IMAGES

At first we present experimental results using the synthetic images. For three different types of 3D structures, we generated the image sequences using the predefined values of intrinsic and extrinsic parameters. We investigated the performance of the algorithm using images with a Gaussian noise. All the results are from error statistics after 100 trials at each noise level. Fig. 1 and Fig. 2 compare the estimated initial value by the proposed method with that of Bougnoux [8]. In Fig. 1, D.C. represents the Degenerated Case when the square root term in Eq. (11) has a negative value or the denominator becomes zero. In the simulation, the proposed initialization method gives no degenerated cases. Also the proposed method gives better initial values when the noise level is smaller than 0.8.

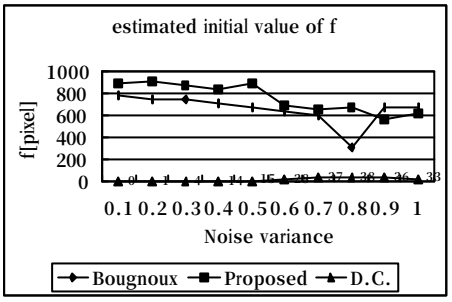

(a)

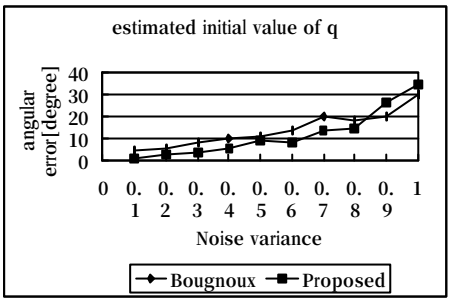

(b)

Fig. 1. The variation of initial value of (a) f and (b) **q** obtained from the method by Bougnoux [8] and the proposed method with respect to the noise variance.

We could not always obtain the meaningful solution in the simulation when the noise level is greater than some values using the original two constraints in Eq. (8). But in these cases the residual in the projective reconstruction remains small and the residual of minimization function decreased too. This is due to the sensitivity of the constraints, which is a 4th order polynomial, to the noise. Fig. 2 represents the result using the original two constraints. We evaluated the accuracy of the estimated solution by comparing the values of f and **q** with those of true ones. True value of **q** can be obtained using Eq. (4) by the transformation matrix between the true projective and metric structures. We represent the error of the estimated **q** vector by the angular difference with the true one. Fig. 2 shows the estimated mean value, the minimum and maximum value at a fixed noise level. We found from the analysis of experimental results that the estimated principal point varies much when compared to other values. Fig. 3 represents the result when we added a new constraint of Eq. (15). We could obtain consistent results in the simulation and the proposed algorithm gives a better performance.

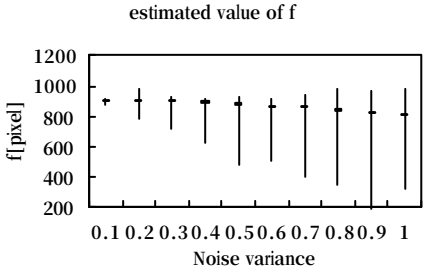

(a)

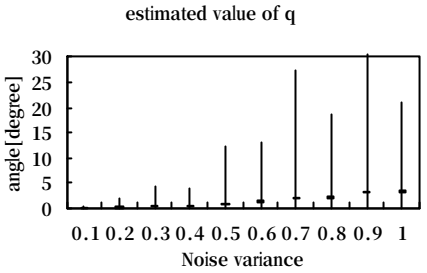

(b)

Fig. 2. The estimated values of (a) *f* (b) **q** when used the original constraints of Eq. (8).

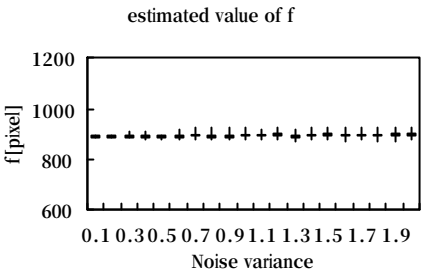

(a)

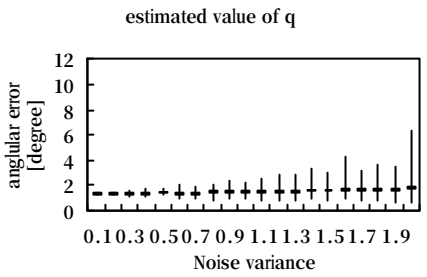

(b)

Fig. 3. The estimated values of (a) f (b) **q** when used additional constraint of Eq. (15).

Next we present the performance of the new linear initialization method using the additional constraint in the self-calibration algorithm. We used a synthetic image sequence of a 15x15x15cm^3 hexahedron with 27 points on each three planes. Images were taken from six different viewing positions as described in Table 2. We consider a situation where the intrinsic parameters of cameras vary as shown in Table 1. Fig. 4 shows the mean of the relative error of the internal parameters over 30 trials for the sixth camera. The error in the estimates of the intrinsic parameters increases monotonically as the image noise increases.

The mean of the relative error of the external parameters is depicted in Fig. 5. We obtained the rotation and the translation parameters through the decomposition of the estimated Euclidean projection matrix. As in the internal parameters, a similar linear tendency to image noise can be observed.

Fig. 6 represents the accuracy of the method in terms of 3D structure recovery. From the scaled Euclidean structure we estimated the relative error of the angle formed by three adjacent points and the ratio of length between two points.

The accuracy degrades monotonically as the image noise increases.

We can observe that the proposed algorithm can effectively cope with the given situation in spite of the varying internal parameters of camera.

Table 1 The values of intrinsic parameters used in the varying camera image sequences.

	C1	C2	C3	C4	C5	C6
α_u	700	700	730	760	790	820
α_v	700	700	730	760	790	820
u_0	256	256	256	256	256	256
v_0	256	256	256	256	256	256

Table 2 The extrinsic parameters used in the generation of synthetic image sequences

	Rotation (q_x, q_y, q_z) [deg]	Translation (t_x, t_y, t_z) [cm]
C1 - C2	$(7^\circ, -5^\circ, 10^\circ)$	$(2.5, 5.0, 2.5)$
C1 - C3	$(-2^\circ, -10^\circ, -15^\circ)$	$(5.0, -5.0, 5.0)$
C1 – C4	$(3^\circ, -15^\circ, 20^\circ)$	$(7.5, 5.0, 7.5)$
C1 – C5	$(-5^\circ, -20^\circ, -10^\circ)$	$(9.0, -5.0, 9.0)$
C1 – C6	$(-10^\circ, -30^\circ, -15^\circ)$	$(7.0, -8.0, 10.0)$

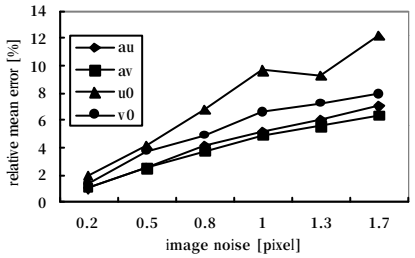

Fig. 4 The relative mean error of the estimated intrinsic parameters of the sixth camera

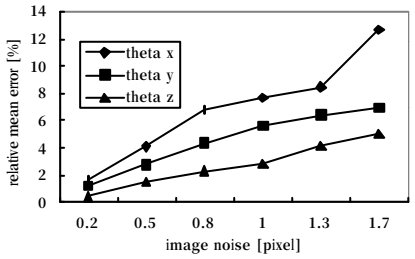

(a)

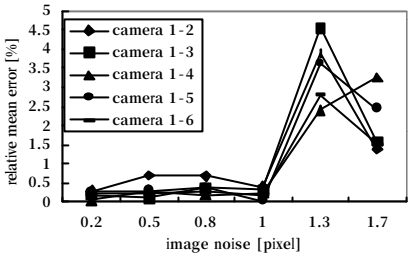

(b)

Fig. 5 The relative mean error of the estimated extrinsic parameter (a) rotation between camera 1 and 6 (b) direction of the translation

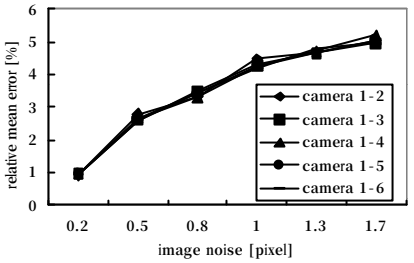

(a)

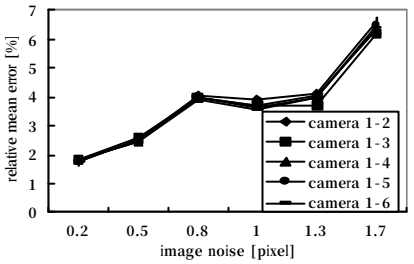

(b)

Fig. 6 The relative mean error of the angle among three points and ratio of length (a) angle among three points (b) ratio of length.

5.2 EXPERIMENTAL RESULTS USING REAL IMAGES

In this section, we present the experimental results using real images. Fig. 7 shows an image sequence of a calibration box used in the experiments. In the experiments we used the cross points on the calibration box to define the correspondence. We compare the quality of estimated structure using the angle between each plane and the ratio of length between points. We obtain the normal vector of the plane after fitting a plane using the estimated Euclidean structure on each plane.

The algorithm using the original two constraints gives angles between each plane as 82.74°, 81.97° and 81.95°. The mean and standard deviation of the ratios of length between horizontal points is 0.4790 ± 0.0266 and between vertical points is 0.4702 ± 0.0200. The ratio of horizontal and vertical length is 1.0187. The proposed algorithm gives angles between each plane as 87.15°, 88.63° and 88.11°. The mean and standard deviation of the ratios of length between horizontal points

is 0.2656 ± 0.0043 and between vertical points is 0.2668 ± 0.0062 . The ratio of horizontal and vertical length is 0.9956. The true angle between each plane is $90^{\square}$ and true value of the ratio of horizontal and vertical length is 1. The proposed algorithm gives much improved results. Fig. 8 shows the estimated Euclidean structure by the proposed algorithm.

Fig. 9 represents an outdoor image sequence captured by a hand-held camcorder. The algorithm using the original two constraints gives the mean and standard deviation of the ratios of length between horizontal points as 0.1321 ± 0.615 and between vertical points as 0.0615 ± 0.0016 . The ratio of the length between the horizontal and vertical lines is 2.14. The proposed algorithm gives 0.0421 ± 0.0012 and 0.0179 ± 0.00046 . The ratio of length between the horizontal and vertical lines is 2.35. The real value of ratio of the length by measurement is 2.48.

The proposed algorithm gives a better quality of Euclidean reconstruction in both experiments.

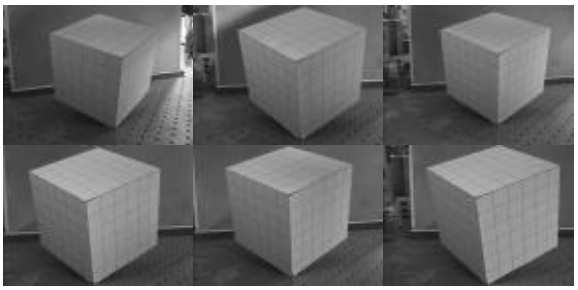

Fig. 7 A real image sequence of a calibration box.

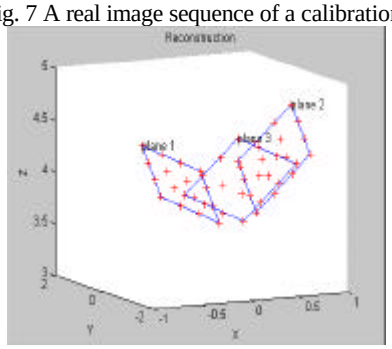

(a)

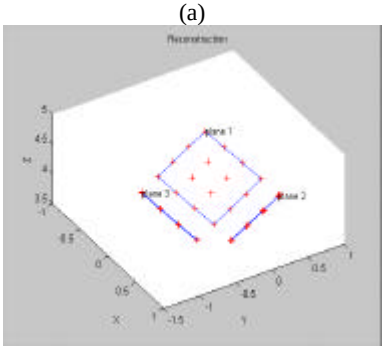

(b)

Fig. 8 A scaled Euclidean structure obtained by the proposed self-calibration algorithm (a) a perspective view; (b) a different view of (a).

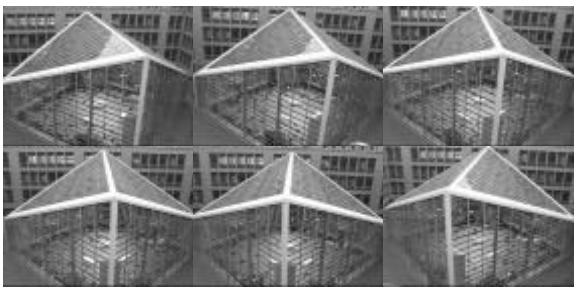

Fig. 9 An input image sequence of an outdoor building.

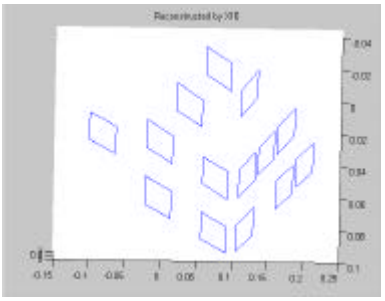

(a)

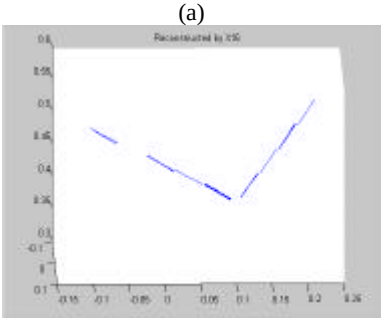

(b)

Fig. 10 The reconstrcuted Euclidean structure by the proposed algorithm (a) a perspective view; (b) another view of (a).

6. CONCLUSIONS

We have presented a practical self-calibration algorithm under varying cameras that only requires a linear projective reconstruction. We also proposed a new linear initialization method for the self-calibration based on the property of the absolute quadric. We improved the performance of self-calibration by adding a new constraint about the position of the principal point. By using this constraint it is possible to use only the linear projective information for practical self-calibration.

REFERENCES

[1] Faugeras, O., Q. -T. Luong, and S. Maybank, "Camera Calibration: Theory and experiments," in *Second European Conference on Computer Vision*, pp.321-334, 1992.

[2] Hartley, R., "Euclidean reconstruction from uncalibrated views," in *Applications of invariance in Computer Vision*, LNCS 825, Springer-Verlag, 1994.

[3] Pollefeys, M. and L. Van Gool, and A. Oosterlinck, "The Modulus Constraint: A New Constraint for

Self-Calibration," in *Proc. ICPR'96*, pp.349-353, 1996.

[4] Heyden, A. and K. Åström, "Euclidean Reconstruction from Constant Intrinsic Parameters," in *Proc. International Conference on Pattern Recognition*, 1996.

[5] Triggs, B., "The Absolute Quadric," in *Proc. Computer Vision and Pattern Recognition*, 1997.

[6] Pollefeys, M. and L. Van Gool, "Self-calibration from the absolute conic on the plane at infinity," in *Proc. CAIP'97*, 1997.

[7] Heyden, A. and Åström, K. "Euclidean Reconstruction from Image Sequences with Varying and Unknown Focal Length and Principal Point," in *Proc. CVPR'97*, 1997.

[8] Bougnoux, S., "From Projective to Euclidean Space under any practical situation, a criticism of self-calibration," *Proc. ICCV'98*, pp.790-796, 1998.

[9] Pollefeys, M., R. Koch, and L. Van Gool, "Self-calibration and Metric Reconstruction in Spite of Varying and Unknown Internal Camera Parameters," in *Proc. ICCV'98*, pp.90-95, 1998.

[10] Faugeras, O., "What can be seen in three dimensions with an uncalibrated stereo rig?" in *Proc. ECCV'92*, pp.563-578, 1992.

[11] Hartley, R., R. Gupta, and T. Chang, "Stereo from uncalibrated cameras," in *Proc. CVPR'92*, pp.761-764, 1992.

[12] Faugeras, O., *Three-Dimensional Computer Vision*, MIT Press, 1993.

[13] Hartley, R. I., "In Defense of the 8-point algorithm," in *Proc. ICCV'95*, pp.1064-1070, 1995.

[14] Csurka, G. and R. Horaud, "Finding the Collineation Between two Projective Reconstruction," *INRIA RR-3468*, 1998.